



## Stability and radioactive gaseous iodine-131 retention capacity of binderless UiO-66-NH<sub>2</sub> granules under severe nuclear accidental conditions

Maeva Leloire, Jérémy Dhainaut, Philippe Devaux, Olivia Leroy, Hortense Desjonqueres, Stéphane Poirier, Philippe Nerisson, Laurent Cantrel, Sébastien Royer, Thierry Loiseau, et al.

### ► To cite this version:

Maeva Leloire, Jérémy Dhainaut, Philippe Devaux, Olivia Leroy, Hortense Desjonqueres, et al.. Stability and radioactive gaseous iodine-131 retention capacity of binderless UiO-66-NH<sub>2</sub> granules under severe nuclear accidental conditions. *Journal of Hazardous Materials*, 2021, 416, pp.125890. 10.1016/j.jhazmat.2021.125890 . hal-03217786

**HAL Id: hal-03217786**

**<https://hal.univ-lille.fr/hal-03217786>**

Submitted on 5 May 2021

**HAL** is a multi-disciplinary open access archive for the deposit and dissemination of scientific research documents, whether they are published or not. The documents may come from teaching and research institutions in France or abroad, or from public or private research centers.

L'archive ouverte pluridisciplinaire **HAL**, est destinée au dépôt et à la diffusion de documents scientifiques de niveau recherche, publiés ou non, émanant des établissements d'enseignement et de recherche français ou étrangers, des laboratoires publics ou privés.



Distributed under a Creative Commons Attribution - NonCommercial - NoDerivatives 4.0 International License

Stability and radioactive gaseous iodine-131 retention capacity of binderless UiO-66-NH<sub>2</sub> granules under severe nuclear accidental conditions

Maëva Leloire, Jérémy Dhainaut, Philippe Devaux, Olivia Leroy, Hortense Desjonqueres, Stéphane Poirier, Philippe Nerisson, Laurent Cantrel, Sébastien Royer, Thierry Loiseau, Christophe Volkringer



PII: S0304-3894(21)00854-2

DOI: <https://doi.org/10.1016/j.jhazmat.2021.125890>

Reference: HAZMAT125890

To appear in: *Journal of Hazardous Materials*

Received date: 25 January 2021

Revised date: 9 April 2021

Accepted date: 10 April 2021

Please cite this article as: Maëva Leloire, Jérémy Dhainaut, Philippe Devaux, Olivia Leroy, Hortense Desjonqueres, Stéphane Poirier, Philippe Nerisson, Laurent Cantrel, Sébastien Royer, Thierry Loiseau and Christophe Volkringer, Stability and radioactive gaseous iodine-131 retention capacity of binderless UiO-66-NH<sub>2</sub> granules under severe nuclear accidental conditions, *Journal of Hazardous Materials*, (2021) doi:<https://doi.org/10.1016/j.jhazmat.2021.125890>

This is a PDF file of an article that has undergone enhancements after acceptance, such as the addition of a cover page and metadata, and formatting for readability, but it is not yet the definitive version of record. This version will undergo additional copyediting, typesetting and review before it is published in its final form, but we are providing this version to give early visibility of the article. Please note that, during the production process, errors may be discovered which could affect the content, and all legal disclaimers that apply to the journal pertain.

# Stability and radioactive gaseous iodine-131 retention capacity of binderless UiO-66-NH<sub>2</sub> granules under severe nuclear accidental conditions

Maëva Leloire,<sup>1,3</sup> Jérémy Dhainaut,<sup>1</sup> Philippe Devaux,<sup>1</sup> Olivia Leroy,<sup>3</sup> Hortense Desjonqueres,<sup>4</sup> Stéphane Poirier,<sup>4</sup> Philippe Nerisson,<sup>3</sup> Laurent Cantrel,<sup>3</sup> Sébastien Royer,<sup>1</sup> Thierry Loiseau,<sup>1</sup> Christophe Volkringer<sup>1,2\*</sup>

AUTHOR ADDRESS.

<sup>1</sup>Univ. Lille, CNRS, Centrale Lille, Univ. Artois, UMR 8181 - UCCS - Unité de Catalyse et Chimie du Solide, F-59000 Lille, France.

<sup>2</sup>Institut Universitaire de France, 1 rue Descartes, 75231 Paris Cedex 05, France.

<sup>3</sup>Institut de Radioprotection et de Sûreté Nucléaire (IRSN), PSN-RES/SEREX, Saint-Paul Lez Durance, 13115, France.

<sup>4</sup>Institut de Radioprotection et de Sûreté Nucléaire (IRSN), PSN-RES/SCA, Gif sur Yvette, 91192, France.

## ABSTRACT

In the present work, we aim to investigate the ability of the zirconium-based MOF-type compound UiO-66-NH<sub>2</sub>, to immobilize molecular gaseous iodine under conditions analogous to those encountered in an operating Filtered Containment Venting System (FCVS) line. Typically, the UiO-66-NH<sub>2</sub> particles were exposed to <sup>131</sup>I (beta and gamma emitters) and submitted to air/steam at 120°C, under gamma irradiation (1.9 kGy.h<sup>-1</sup>).

In parallel to this experiment under simulated accidental conditions, the stability of the binderless UiO-66-NH<sub>2</sub> granules under steam and gamma irradiation was investigated. In order to fit with the specifications required by typical venting systems, and to compare the efficiency of the selected MOF to porous materials commonly used by the industry, scale-up

syntheses and UiO-66-NH<sub>2</sub> millimetric-size shaping were realized. For this task, we developed an original binderless method, in order to analyze solely the efficiency of the UiO-66-NH<sub>2</sub> material. The shaped MOF particles were then submitted separately to gamma irradiation, steam and temperature, for confirming their viability in a venting process. Their structural, textural and mechanical behaviors were characterized by the means several techniques including gas sorption, powder X-ray diffraction, infrared spectroscopy and crushing tests. Promising results were obtained to trap gaseous molecular iodine in severe accidental conditions.

## KEYWORDS

Nuclear severe accident, gaseous iodine-131, immobilization, Metal-Organic Framework, UiO-66-NH<sub>2</sub>.

## 1. INTRODUCTION

During a core melt accident, the production of large amounts of gas (steam, hydrogen) combined with volatile radionuclides (iodine derivatives, noble gases) are likely to be released, increasing the pressure inside the nuclear containment building. In the absence of an effective depressurization setup, the concrete containment structure can be irreversibly damaged by a high overpressure, leading to a loss of confinement with large direct leakages to the environment promoting outside radiotoxic species. Thus, containments are equipped with containment venting system (CVS) which can be filtered or not. This scenario happened at Fukushima Daichi nuclear plant, when an accidental discharge of contaminated steam/hydrogen induced an over-pressurization and the explosion of 3 reactor buildings.<sup>1</sup> Whereas this nuclear plant was not equipped with a filtering device, the existing venting system was broken down due to the earthquake and the tsunami which occurred just before. And while the manual venting was activated relatively early, it did not avoid the explosion (mainly due to hydrogen) and further releasing of radioactive species. Among them, iodine isotopes are of particular interest (mainly <sup>129</sup>I, <sup>131</sup>I and <sup>133</sup>I), since they can be adsorbed in thyroid hormones, responsible for the regulation of metabolism, therefore disseminating the radiotoxicity in the whole body.

To remediate this situation, the nuclear industry has developed for decades sophisticated mitigation technologies, especially the Filtered Containment Venting System (FCVS).<sup>2</sup> This

equipment is particularly attractive, since it is based on a passive process that does not depend on any external input. Furthermore, this venting setup is associated to a filtration step providing retention of radioactive products (aerosols and some gases). Usually, FCVS consists of a combination of wet or dry filtration procedures (such as metallic filters, aqueous scrubbers, sand bed filters). An additional filtration line involving inorganic porous adsorbent, mainly silver doped zeolites, can also be implemented,<sup>3</sup> to selectively trap organic iodides which may contribute to high radiological consequences. Whereas these microporous solids are very efficient for the immobilization of iodine and/or the decomposition of organic iodides,<sup>4-7</sup> their relatively low porosity limits the diffusion of bulky radioactive molecules such as iodine derivatives ( $I_2$ ,  $CH_3I$ )<sup>8</sup> or ruthenium tetroxide ( $RuO_4$ ).<sup>9</sup> Thanks to their superior porosity features, Metal-Organic Frameworks (MOFs) appear as a good alternative for the capture of large amount of iodine.<sup>10</sup> Indeed, these hybrid materials, formed by the association of metallic cations and organic ligands, can exhibit much higher pore diameters (up to 98 Å)<sup>11</sup> and specific surface areas (up to 7100 m<sup>2</sup>/g-BET model)<sup>12</sup> than those commonly reported for zeolites (around 10 Å and 1000 m<sup>2</sup>/g, respectively). Whereas MOFs exhibit lower thermal resistance than pure inorganic porous materials, their uses in a venting system is possible. Indeed, the thermal behavior of these hybrid materials is mainly commanded by the stability of the organic ligand, which usually starts to decompose above 300 °C.<sup>13</sup> This temperature limit remains much higher than the temperature inside the dry FCVS which is lower than 200°C, the heating results from overheated steam and decay heats of fission products trapped. During a severe accident, the fuel cooling is lost and water cooling the reactor is vaporized. Most of MOFs are well known to be highly sensitive to water. Indeed, coordination of water molecules with metallic cations leads to the hydrolysis of the chemical bond bridging the metallic cations to the ligands.<sup>14</sup> However, above 100 °C, adsorption of water over MOF surface is inhibited, thus preventing structural decomposition.<sup>15</sup> Finally, recent studies also proved the very good stability of selected MOFs versus ionizing radiations such as gamma ray.<sup>16,17</sup> In this last case, the resistance is assigned to the very low density of MOFs, limiting the interaction with the electromagnetic radiation.

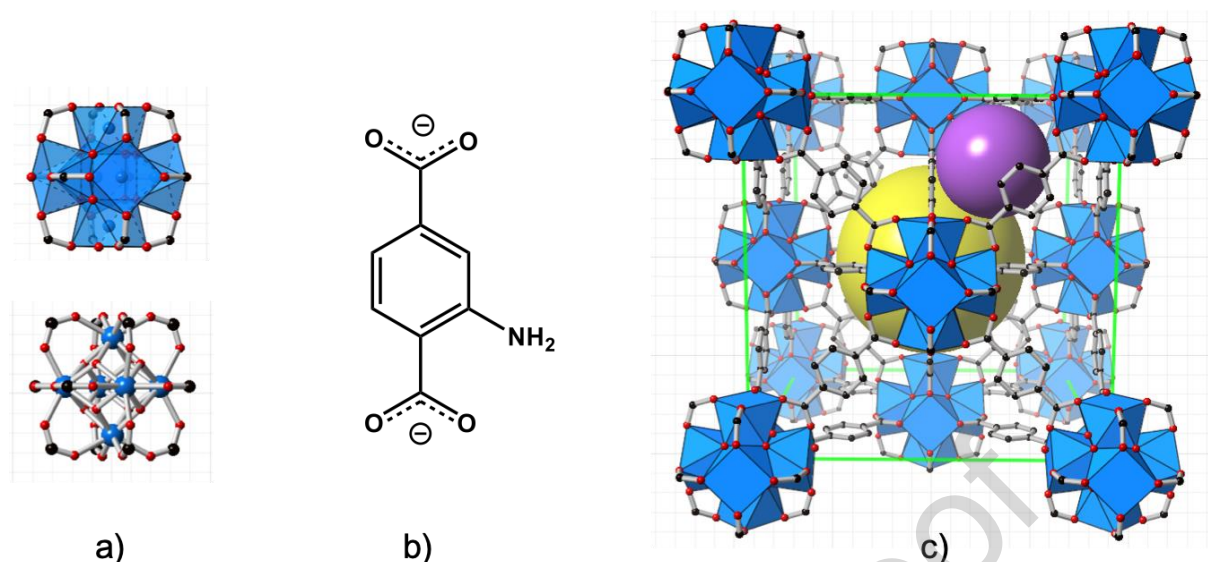


**Figure 1.** Structure of UiO-66-NH<sub>2</sub>. Polyhedral and “ball and stick” views of the hexanuclear Zr<sub>6</sub> cluster (a), aminoterephthalate ligand (b) and perspective view of the crystal structure of UiO-66-NH<sub>2</sub> (c). Yellow and purple spheres indicate the spaces of octahedral and tetrahedral cavities, respectively.

Several studies already proved the great efficiency of some MOFs for the capture and the immobilization of molecular iodine.<sup>10</sup> The affinity of iodine with the structure can be optimized by the selection of appropriate pore diameters fitting with the diameter of I<sub>2</sub><sup>18</sup> or by the presence of electro-donor chemical groups (i.e. -NH<sub>2</sub>) onto the MOF framework,<sup>19</sup> in order to generate a stable charge-transfer complex with iodine.<sup>20</sup> Afterwards, the powdered solids charged with iodine can undergo post-treatments, like amorphization<sup>21</sup> or sintered with glass matrices,<sup>22</sup> in order to guarantee the long term confinement of volatile iodine. Although MOFs show a great potential for utilization in a FCVS-like equipment, their efficiency needs to be confirmed under simulated accidental conditions (i.e. irradiation, steam, high temperature).

UiO-66-NH<sub>2</sub>, which can be prepared in water from commercially-available reagents,<sup>23</sup> combines several of these last advantages, making that MOF a great candidate for the sorption and the immobilization of radionuclides in the case of a nuclear accident. Moreover, its high thermal and chemical stabilities make this solid potentially usable under drastic conditions.<sup>24, 25</sup> All of these make UiO-66-NH<sub>2</sub> very attractive for large scale, industrial applications in filtration processes and justify the choice of this material in this work. Herein, its affinity for iodine will be confirmed in this work, through the evaluation of iodine uptake

under severe conditions mimicking a nuclear accident, and compared to silver-doped zeolite which is currently used by the nuclear industry.

In the present work, we aim to investigate the ability of the zirconium-based UiO-66-NH<sub>2</sub> material (Fig. 1),<sup>26</sup> to immobilize gaseous molecular iodine under conditions analogous to those encountered in an operating FCVS line. Typically, the UiO-66-NH<sub>2</sub> particles were exposed to <sup>131</sup>I (beta and gamma emitters) and submitted to air/steam at 120°C, under gamma irradiation (1.9 kGy.h<sup>-1</sup>). Gaseous iodine release was followed *in situ* by gamma spectrometry.

UiO-66 is a prototypical MOF structure, where Zr-based hexanuclear clusters are connected to each other by terephthalate ligands.<sup>27</sup> The 3D network adopts a face-centered cubic (*fcc*) topology, containing tetrahedral and octahedral cavities with an estimated diameter of 7 Å and 12 Å, respectively. In UiO-66-NH<sub>2</sub>, terephthalate ligands are pre-functionalized by an accessible amine group (-NH<sub>2</sub>),<sup>26</sup> which favors the affinity for iodine.<sup>19</sup>

In parallel to this experiment under simulated severe accidental conditions, the stability of the binderless MOF granules under steam and gamma irradiation was investigated. In order to fit with the specifications required by typical venting systems, and to compare the efficiency of the selected UiO-66-NH<sub>2</sub> to porous materials commonly used by the industry, scale-up syntheses and millimetric-size shaping were realized. For this task, we developed an original binderless method, in order to analyze solely the efficiency of the UiO-66-NH<sub>2</sub> material. The shaped UiO-66-NH<sub>2</sub> particles were then submitted separately to gamma irradiation, steam and temperature, for confirming their viability in a venting process. Their structural, textural and mechanical behaviors were characterized by the means several techniques including gas sorption, powder X-ray diffraction, infrared spectroscopy and crushing tests. The studies involving gaseous <sup>131</sup>I radioisotope and gamma irradiation was realized in specific facilities from the French Institute of Radiological Protection and Nuclear Safety (IRSN).

## 2. EXPERIMENTAL

### 2.1. Chemicals and materials

Zirconium chloride (ZrCl<sub>4</sub>, 99.5%, from Alfa Aesar), 2-aminoterephthalic acid (H<sub>2</sub>BDC-NH<sub>2</sub>, 99.0%, from Alfa Aesar), formic acid (HCOOH, 99.9%, from Acros Organics),



dimethylformamide (DMF, 98%, from Fisher Scientific), methanol (98%, VWR), ethanol (96%, VWR), Labelled  $^{131}\text{I}$  ( $\text{Na}^{131}\text{I}$  in 0.1 M NaOH, 3.7 kBq-3.7 MBq from Perkin Elmer), Sodium iodide (NaI 99.5% from Prolabo), Sodium iodate ( $\text{NaIO}_3$ , 99.0% from Acros)

## 2.2. UiO-66-NH<sub>2</sub> scale-up synthesis

Two scale-up synthesis methods were utilized during this study.

In a first method, UiO-66-NH<sub>2</sub> was synthesized in a Schott DURAN® pressure plus bottle with a volume of 1L under static conditions. 16 g of  $\text{ZrCl}_4$  and 24 g of  $\text{H}_2\text{BDC-NH}_2$  were added to a mixture of DMF (650 ml) and  $\text{HCOOH}$  (130 ml). The resulting solution was heated in static conditions at 120 °C during 24 h. The solid was then collected by centrifugation and redispersed in 1 L of fresh DMF during 24 h (3 times) and then in fresh methanol during 24 h (3 times). After centrifugation the solid was dried during 1 h at 100 °C and then 8 h at 150 °C. Each synthesis gave approximately 17 g of product (yield based on Zr: 75 wt.%), and 12 syntheses were necessary to produce a unique batch of 200 g of UiO-66-NH<sub>2</sub> powder (batch 1). After shaping process, batch 1 was used for experiments involving resistance of binderless-shaped MOFs under steam and iodine immobilization under accidental conditions.

The second large-scale synthesis method utilized a 10 L stainless-steel autoclave (Top Industrie, Fig. S2), where 80 g of  $\text{ZrCl}_4$  and 120 g of  $\text{H}_2\text{BDC-NH}_2$  were added to a solution of DMF (3.25 L) and  $\text{HCOOH}$  (0.65 L). The mixture was agitated (100 rpm) during 24 h at 120 °C. Then, the solid was separated from the supernatant by centrifugation and the resulting product was submitted to the same activation as mentioned above. Each batch gave 88 g of product (yield based on Zr: 88 wt.%), and two batches were blended to produce a unique batch of 176 g (batch 2). After shaping process, batch 2 was used for experiments devoted to the chemical behavior study of binderless-shaped MOF under gamma irradiation.

## 2.3. UiO-66-NH<sub>2</sub> shaping process

A binderless wet granulation method was developed for the purpose of this study. The different equipment used for the process are presented in supplementary information (Fig. S3). For the shaping, 200 g of dry UiO-66-NH<sub>2</sub> powder were added in the mixing pan of a high shear EL1 granulation mixer (Eirich). The mixing pan was rotated clockwise at 60 rpm, while the stirring rotor was rotated anticlockwise at 900 rpm for 300 s. During this rotation,



portions of a 50/50 mixture of water/ethanol (v/v) were added until reaching 100 mL. After 450 s, the rotation speed of the stirring rotor was increased to 1200 rpm, and additional 80 mL of the water/ethanol mixture were added. The resulting granules were sieved for separating different grain sizes. Granules with spherical diameter in the range 0.5 to 1.4 mm were collected and spheronized on a rotating pan (ERKAWA) at 150 rpm for 3 h. After a second sieving step, the grains were dried overnight at 60 °C, then 24 h at 100 °C. About 150 g of UiO-66-NH<sub>2</sub> granules, with spherical diameters ranging from 0.5 to 1.4 mm, were thus obtained.

## 2.4. Stability experiments

### 2.4.1 Under steam

A controlled amount of steam was produced by a Vapor Delivery Module (VDM Serie Bronkhorst, Fig. S1), involving a controlled evaporation and a mixing system, connected to a pressurized water tank of 1 L. Argon was used as single carrier gas. The flows of argon and liquid water were adjusted to 15 L<sub>n</sub>.h<sup>-1</sup> and 5 g.h<sup>-1</sup>, respectively. The latter corresponds to the maximal output capacity of the module used in this study. These process conditions correspond to a volume fraction of steam in argon of 29 % at 1.5 bar (absolute) with a relative humidity (RH) of 99 % at a dew point of 78 °C.

For the analysis of MOF stability, the glass reactor was filled with 500 mg of dried UiO-66-NH<sub>2</sub> granules. Prior to the experiment, the porous material bed was flushed with argon during 10 min in order to evacuate physisorbed H<sub>2</sub>O. The temperature inside the reactor, measured with a K-type thermocouple, was set to 80°C. Steam production was initiated when the targeted temperature was stabilized. Immediately after the end of the experiment, UiO-66-NH<sub>2</sub> granules were quickly transferred into a glove box inerted with argon, in order to prevent further exposure to moisture from ambient air.

### 2.4.2 Under gamma irradiation using IRMA facility

UiO-66-NH<sub>2</sub> samples were submitted to 1 MGy and 2 MGy doses, within the gamma irradiation cell called IRMA (IRradiation MAterials, Fig. S4) of the IRSN located at Saclay research center. IRMA is a panoramic irradiation cell for studying how materials or equipment react to the effects of dose and dose rate due to exposure to gamma radiation (Fig. 2).

The research facility hosts four cylindrical sealed sources of cobalt-60 ( $T_{1/2} = 5.27$  years), totaling 817 TBq right before the experiments presented in this work (May 2019). At the date of the tests, the dose rate was approximately 12 kGy/h at 10 cm from the plot containing the four sources.

The calculation of the theoretical distances between the sources and the vials containing UiO-66-NH<sub>2</sub> granules under test were realized using a dedicated software (Microshield® 9.07 software), which simulates the dose rate absorbed by air at the material samples or equipment locations.

The theoretical distances are validated by measuring the dose rate (air equivalent) using a calibrated ionization chamber (chamber of 0.125 cm<sup>3</sup>, in order to measure dose rates in the range from 9 Gy/h to 8 kGy/h ranges) at the location of the experimental mock-ups (empty glass bottle), representative of the material under gamma irradiation (Fig. S4).

The radioactive sources were remotely handled after withdrawal from their safe repository (lead castle). The required number of <sup>60</sup>Co sources were then positioned in order to deliver the targeted dose rate to the items to be tested during a predetermined time (hence, the programmed dose).

Then, a closed glass bottle containing dried UiO-66-NH<sub>2</sub> granules was placed on a planar sample holder at 13.6 cm from the four <sup>60</sup>Co sources (Fig. 2). For this experiment, the dose rate was 6.94 kGy/h (exposition during 292 hours) for an integrated dose of 2030 KGy. At the halfway through the test (144 hours), the bottle was 180° rotated for a homogeneous irradiation.

At the end of the experiment, the irradiated UiO-66-NH<sub>2</sub> beads were transferred into a glove box to avoid any contamination with water.



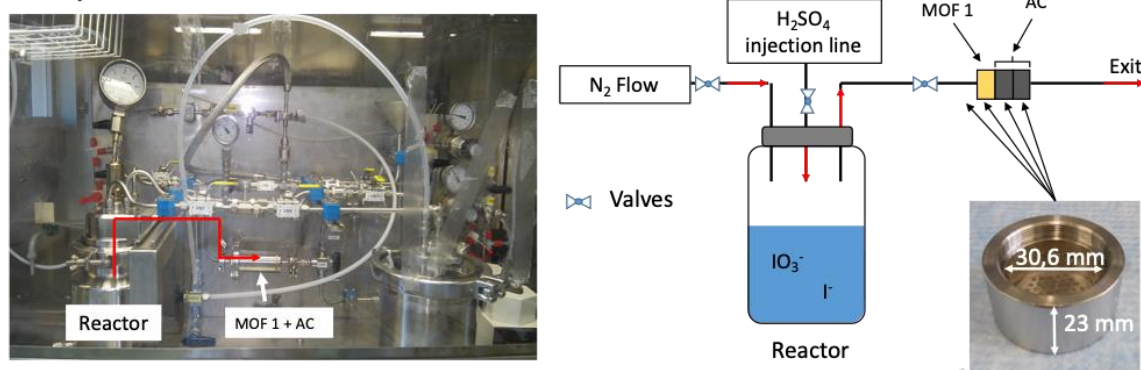
**Figure 2.** Interior photograph of the IRMA irradiator cell (left) and vial organization around dummy  $^{60}\text{Co}$  sources (right).

#### 2.4.3 Iodine retention under radioactive conditions using EPICUR facility

The EPICUR facility (Fig. 3) is a panoramic irradiator, part of the IRSN CHROMIA platform (Cadarache, France), dedicated to the behavior of fission products in accidental conditions containing  $^{60}\text{Co}$  sources and designed to deliver an average dose of  $1.9 \text{ kGy.h}^{-1}$  (for this study). It is usually used to study the behavior of iodine under irradiation, and reproduce the conditions that could be encountered in a reactor building during a nuclear accident.

In this study, EPICUR facility was used in order to evaluate the capacity of UiO-66- $\text{NH}_2$  to immobilize molecular iodine within their framework. This experiment is decomposed in two steps (Fig. 3). The first one (Fig. 3, step 1) consists in the production of labelled radioiodine ( $^{131}\text{I}$  isotope) and its capture by the UiO-66- $\text{NH}_2$  sample shaped from batch 1. The second one (Fig. 3, step2) is to measure during the irradiation phase, the possible releases of labelled iodine ( $^{131}\text{I}$ ) under accidental conditions.

## Step 1:



## Step 2:

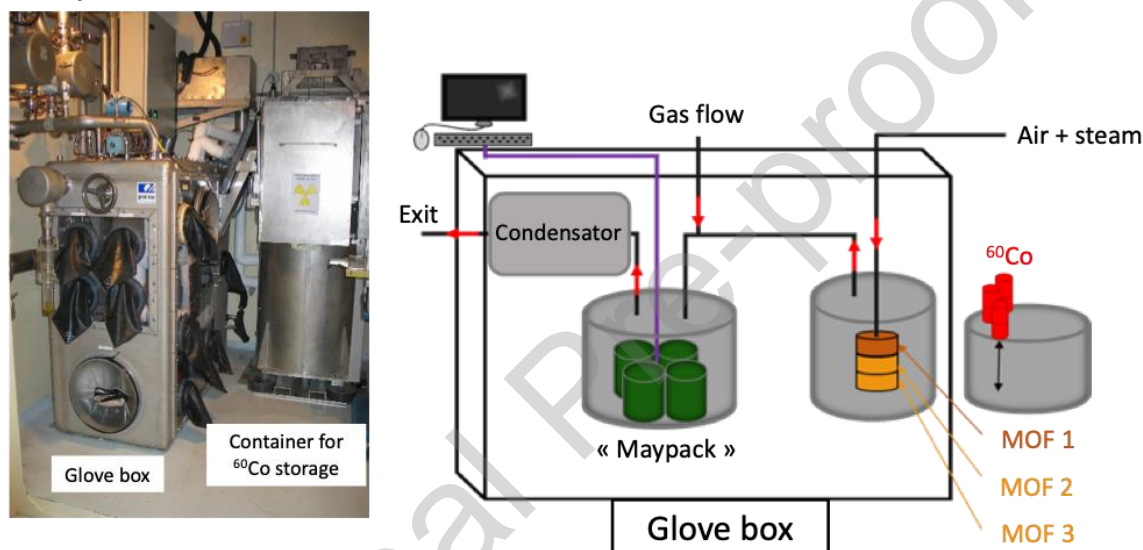
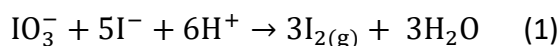


**Figure 3.** Experiments performed using EPICUR setup. Top: Photography (left) and scheme (right) of the installation for the iodine adsorption of MOFs (step 1). Insert: Photography of an adsorbent holder. Bottom: Photography (left) and scheme (right) of the EPICUR facility.

UiO-66-NH<sub>2</sub> (3.4 g) was placed into a stainless steel cylindric holder (called MOF 1, Fig. 3) of diameter 30.6 mm and thickness 23 mm. Downstream, two additional holders were filled with activated charcoal, in order to prevent any loss of radioiodine (<sup>131</sup>I) during the loading step. Afterwards, the reactor was closed and connected to the vessel, where the gaseous iodine is generated by the Dushman's reaction.

Based on the Dushman's reaction (eq. 1),<sup>29</sup> gaseous radioactive molecular iodine was produced at 50°C from a solution containing a mixture of NaI/NaIO<sub>3</sub> in presence of radioactive iodine used for labelling (<sup>131</sup>I, pH ≈ 7) and acidified with sulfuric acid to reach a final pH = 3.



Molecular iodine  $I_2$  was transported by air flow through the MOF holder at a velocity of  $59 \text{ cm.s}^{-1}$  (flow rate of  $26 \text{ L.min}^{-1}$ ). The generation of gaseous iodine is stopped by adding 50 mL of NaOH ( $0.1 \text{ mol.L}^{-1}$ ), in order to bring the solution at  $\text{pH} > 11$ . The radioiodine loading into the MOF holders was then measured by gamma spectrometry (using NaI(Tl) scintillator and Interwinner – Itech Software). Accurate measurement of gaseous radioiodine activity in the two MOF holders were achieved owing to internal calibration.

After this first step, the loaded MOF holder (MOF 1) was supplemented downstream by two other holders containing non-iodine loaded MOF granules (MOF 2 and MOF 3), placed in a stainless-steel irradiation vessel, and connected through stainless-steel tubes to an iodine supporting filtration system, called Maypack (step 2). Temperature, pressure and gaseous atmosphere composition are controlled in the irradiation vessel. During a pre-irradiation phase of 7 h, the vessel was heated to the targeted temperature ( $120^\circ\text{C}$ ) and pressure ( $3.5 \text{ bar abs.}$ ), under a flow of wet air with relative humidity (R.H.) of 20 % and a space velocity of  $0.9 \text{ cm.s}^{-1}$ . During the irradiation phase (30h, dose rate of  $1.9 \text{ KGy.h}^{-1}$ ), the temperature and the pressure within the vessel were maintained at  $120^\circ\text{C}$  and  $3.5 \text{ bar abs.}$ , respectively. The air and steam flows were fixed to  $68.8 \text{ g.h}^{-1}$  and  $5.5 \text{ g.h}^{-1}$  (20 % R.H.), respectively. After the irradiation phase, the irradiation vessel was outgassed under wet air during 5 hours and dried under air during 1 hour.

The volatile species released by radiation and thermal constraints in the irradiation vessel are transferred to the Maypack device (Fig. 3). This section is composed of 3 filters able to trap selectively iodine aerosols (Quartz Fiber filter), inorganic iodine (Knit-mesh filter with silver clad copper) and organic iodides R-I (KI impregnated charcoal filter). Continuous  $\gamma$ -measurements were performed on the Maypack device, in order to follow the amount of radioactive species released by the UiO-66- $\text{NH}_2$  granules. At the end of the irradiation phase, the MOF holders, the Maypack filters and the washing solutions were  $\gamma$ -counted, in order to evaluate the iodine release. The post-tests measurements were used to correct the online measurements.  $\gamma$ -measurement uncertainties are estimated to be 10%.

## 2.5. Characterization

The powder X-ray diffraction (PXRD) patterns of the different compounds were registered at RT by using a Bruker D8 Advance A25 diffractometer with Bragg-Brentano geometry ( $\theta$ - $2\theta$

mode), ranging from 3 to 50° ( $2\theta$ ), a step length of 0.02° ( $2\theta$ ) and a counting time of 0.5 s/step. The D8 system was equipped with a LynxEye detector with CuK $\alpha$  radiation.

N<sub>2</sub> adsorption isotherms were recorded at 77K using a Micromeritics ASAP2020 apparatus. Specific surface area was calculated in the P/P<sub>0</sub> range: 0.015–0.30 using the BET method. Before sorption measurements, the sample was outgassed under primary vacuum (5 Pa) at 120°C for 15 h.

IR spectra were measured on a Perkin–Elmer Spectrum Two spectrometer equipped with a diamond attenuated total reflectance (ATR) accessory between 4000 and 400 cm<sup>-1</sup>.

The ultimate strength of MOF granules, as-prepared and after application of severe conditions, was evaluated using a Catalyst Crushing Strength Tester (Vinci Technologies). For each series, 10 granules were compressed at a constant speed of 10  $\mu\text{m.s}^{-1}$  until observation of the fracture on the stress-strain curve.

## RESULTS AND DISCUSSION

### UiO-66-NH<sub>2</sub> binderless shaping

Finely-divided powders are not adapted to an emergency filtration setup located in a nuclear plant. Indeed, the suspension of such fine particles in air, during filters replacement, could provoke an important dust explosion. Furthermore, compaction of powder in the presence of humidity can lead to the obstruction of filters and a dangerous increase of pressure throughout the filtration line.<sup>30</sup> Finally, powders are uneasy to manipulate and recover. In this work, we chose to produce millimetric granules following binderless wet granulation approach, a strategy not reported to date.<sup>31, 32</sup> The absence of any binder was preferable to analyze the performance of UiO-66-NH<sub>2</sub> exclusively as well as to avoid increased sensitivity of the granules versus gamma rays due to the presence organic binder additives.

Prior to UiO-66-NH<sub>2</sub> granules production, large scale syntheses were carried out in order to provide the adequate quantity of MOF powder needed (> 100 gr).

After their synthesis, UiO-66-NH<sub>2</sub> in batches 1 and 2 exhibit pure and well-defined powdered X-ray diffraction patterns (Fig. S10). BET surface areas obtained are slightly lower (756 and 605 m<sup>2</sup>.g<sup>-1</sup>, respectively) than the values usually encountered in the literature for small-scale synthesis (> 800 m<sup>2</sup>/g).<sup>26</sup> This lower porosity can be explained by a lower crystallinity (usual



from large scale synthesis)<sup>33</sup> and the occurrence of traces of remaining DMF solvent still trapped within the pores of UiO-66-NH<sub>2</sub> framework, despite intense activation. The latter was confirmed by infrared spectroscopy, displaying the visible characteristic band of DMF ( $\nu_{\text{C=O}} = 1660 \text{ cm}^{-1}$ ) (Fig. 4). Moreover, another vibration band at  $1686 \text{ cm}^{-1}$  is observed on the powdered sample and can be usually assigned to free carboxylic group, located at the surface of the crystallites. This band disappeared after applying shaping process. These batches were granulated as-such, leading to spherical pale-yellow granules constituted of agglomerates of nanometric UiO-66-NH<sub>2</sub> crystallites (Fig. 5).

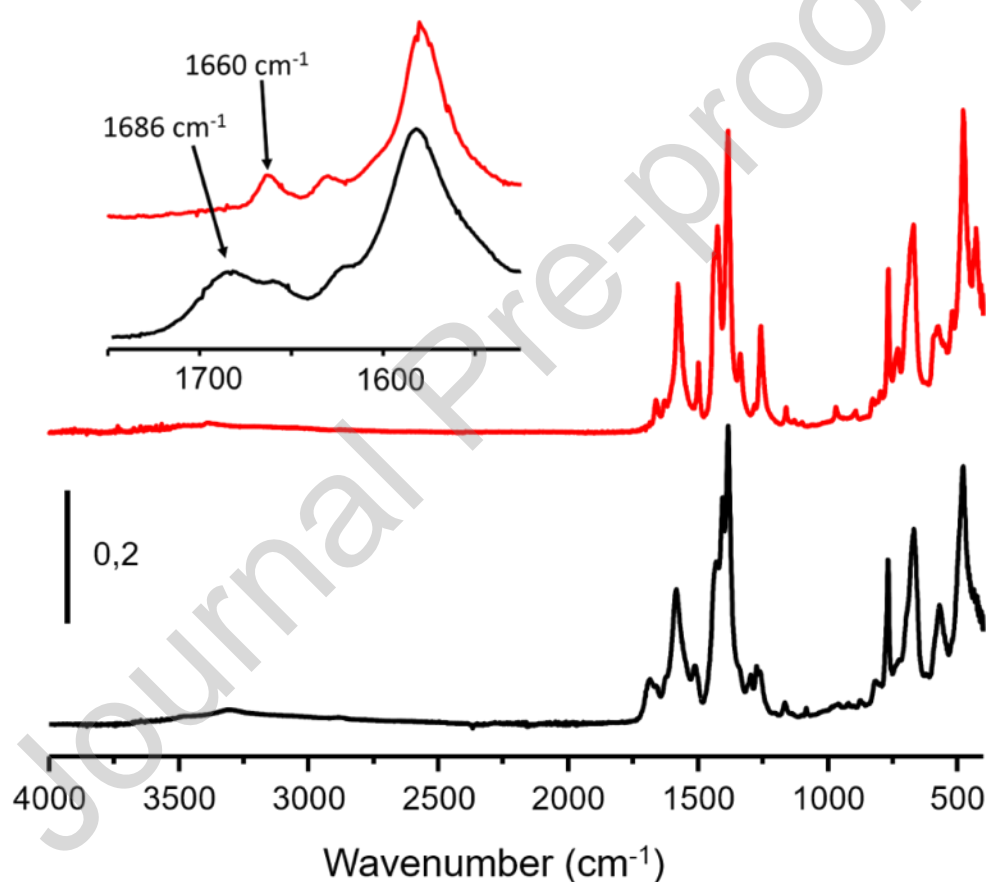


**Figure 4.** Infrared spectra of UiO-66-NH<sub>2</sub> (example of batch 1) collected from powdered (black) and shaped (red) samples and focus on the  $1800\text{-}1500 \text{ cm}^{-1}$  range.

The wet granulation process did not alter the crystallinity since both PXRD patterns (Fig. S11) N<sub>2</sub> isotherms are unchanged, with comparable surface areas calculated (batch 1: 756 vs. 747 m<sup>2</sup>/g, batch 2: 605 vs. 622 m<sup>2</sup>/g). Creation of covalent connections between the MOF crystallites is deduced from IR spectra with the disappearance of the band at  $1686 \text{ cm}^{-1}$  (Fig.



4). This phenomenon can be assigned to the complexation of unsaturated zirconium cations located at the surface of UiO-66-NH<sub>2</sub> crystallites through the free carboxylic functions. Furthermore, the local heating generated by the granulation step, combined with the presence of solvents (ethanol and H<sub>2</sub>O), allows partial extraction of residual DMF, as revealed by the lower intensity of the vibration band at 1660 cm<sup>-1</sup>.



**Figure 5.** Photographs of binderless shaped UiO-66-NH<sub>2</sub> granules, with spherical size in the range 0.5-1.4 mm. From left to right: Pristine, submitted to a 2MGy dose ( $\gamma$  radiation), submitted to water steam (120°C, 7 days), charged with <sup>131</sup>I then submitted to accidental conditions.

The mechanical stability of the granules was evaluated by compression over 10 granules until fracture. The average compressive strength was measured as  $0.3 \pm 0.2$  N and  $0.2 \pm 0.1$  N for batch 1 and batch 2, respectively (Fig. S19-S20). This value is lower than those characterizing MOF bodies containing few percent of a binder, which is found to drastically improve the mechanical strength ( $> 2.5$  N).<sup>31</sup> However the mechanical stability of the binderless UiO-66-NH<sub>2</sub> granules remains sufficient for their manually handling and preparation of adsorbent columns for tests.

#### **Stability of UiO-66-NH<sub>2</sub> under water steam and under gamma irradiation (studied separately):**

A previous study dedicated to the resistance of Cu-based MOF called HKUST-1 under steam showed that its decomposition is maximized for temperatures below or equal to the water boiling point.<sup>15</sup> Under those conditions, the reactivity of water molecules and a direct contact with the material surface are sufficient to rapidly initiate the hydrolysis of the bonds connecting metallic cations to oxo groups from the polytopic carboxylate ligands. Therefore, in this study UiO-66-NH<sub>2</sub> (powder and binderless-shaped granules) was submitted to a water

flow at 100°C (RH of 43.4 %) during 7 days. After this long period, PXRD and SEM microscopy techniques did not indicate any traces of crystallinity loss of either powdered solids or granules (see supplementary information).

Interestingly, whereas steam at 100°C did not affect the crystalline structure of UiO-66-NH<sub>2</sub>, the thermal treatment associated to steam improved the porosity of the solids. Based on the BET surface areas values (Table S1), the porosity gain is 48 % and 41 % for powdered and shaped UiO-66-NH<sub>2</sub> samples, respectively. The lower gain obtained with granules could be explained by their larger size and marked tortuosity, limiting the diffusion rate of water and consequently its effect.

From the isotherm shape obtained after steam treatment that remained of pure type 1, and the infrared spectra changes (decrease of the  $\nu_{C=O} = 1660 \text{ cm}^{-1}$  band after treatment, Fig. S14), the improvement of porosity can be associated to the removal of DMF molecules initially present within the cavity despite the activation process. One supposes that the combination of temperature and steam flowing during seven days favors the removal of organic solvent molecules trapped within the pores. Finally, the steam treatment that resulted in a significant improvement of porosity in the material, did not induced a decrease of the mechanical resistance of the shaped material ( $0.4 \pm 0.2 \text{ N}$  vs.  $0.3 \pm 0.2 \text{ N}$  for the untreated material, Fig S19)

For the powdered sample, the steam medium also allowed reactivity between zirconium cations and free carboxylic functions, as indicated by the disappearance of the band at  $1686 \text{ cm}^{-1}$  on IR spectrum (Fig S14).

After having been submitted to a dose of 2 MGy (IRMA cell), UiO-66-NH<sub>2</sub> granules (batch 2) were not altered keeping their size, a pale-yellow color (Fig. 5), comparable structural organization with associated improved porosity (+ 6%, Table S1). Therefore, the UiO-66-NH<sub>2</sub> compound shows an improved stability versus gamma irradiation compared to the non-functionalized phase.<sup>16, 17</sup> This resistance toward irradiation could be assigned to the ability of scavenger groups, such as amines, to neutralize radicals formed by ionizing radiation<sup>34</sup> and to stop radical reactions accelerating the three dimensional network break. The compressive mechanical strength of UiO-66-NH<sub>2</sub> granules was also unchanged ( $0.2 \pm 0.1 \text{ N}$ ) after gamma irradiation (Fig. S20).

**Stability of iodine trapping under accidental conditions.**

Prior to irradiation tests, UiO-66-NH<sub>2</sub> granules were previously charged with labelled iodine (<sup>131</sup>I<sub>2</sub>), leading to an uptake of 7.8 mg of iodine per gram of MOF (noted 7.8 mg.g<sup>-1</sup>) and corresponding to an initial activity of 4,77x10<sup>5</sup> Bq. This value is comparable to those obtained with silver-doped zeolites using the same loading method,<sup>4</sup> but remains much lower than the maximum capacity expected for an amino-functionalized MOF compounds (>100 mg.g<sup>-1</sup>).<sup>19</sup> This difference is due to the high space velocity used for material I<sub>2</sub> loading (40 cm.s<sup>-1</sup>) associated with the relatively short exposure time (2h) used in this study.

Irradiation tests were performed onto iodine-charged UiO-66-NH<sub>2</sub> granules, in order to check the proper immobilization of molecular iodine within the porous solid, upon simulated accidental conditions (T = 120°C, pressure = 3.5 bar, wet air R.H. = 20%, 30 h of irradiation with a dose rate of 1.9 kGy.h<sup>-1</sup>).

During the test, no trace of iodine was detected in the Maypack device. The iodine was therefore retained in the first holders (MOF 1 + additional MOF 2 and 3) during the whole experiment. After irradiations (<sup>60</sup>Co source), the MOF holders (MOF1, MOF2 and MOF3), the Maypack filters and the rinsing solutions for the experimental device (irradiation vessel and experimental loop) were all gamma-counted (Table 1).

The separate gamma counting of the three holders of UiO-66-NH<sub>2</sub> samples reveals a low activity in the additional MOF3 holder (0.8% of the initial activity of the MOF1 holder). This remark can be explained by two hypotheses, either by a slight release of iodine from the first holder (MOF1) to the next one (MOF2), or by a transfer of MOF fine powder from holder 1 to the next holder (MOF2) under the action of the gas flow. Indeed, the UiO-66-NH<sub>2</sub> grains could undergo a slight surface abrasion under the effect of accidental conditions or the mechanical stress associated with their compaction in the test holder.

**Table 1.** Activities of the different components of the filtration line. The activities are expressed in % of initial activity of holder MOF1. QL : quantification limit, 100 Bq

Initial activity in holder MOF1 (Bq)	4,77x10 <sup>5</sup>
Final activity in holder MOF1 - after irradiation (%)	99,3
Final activity in holder MOF2 (%)	0,79
Final activity in holder MOF3 (%)	< QL
Quartz filter fiber (aerosols) (%)	< QL
knit-mesh (molecular iodine) (%)	< QL
Active charcoal (organic iodine) (%)	< QL
Rinsing solution (%)	0,7
Iodine balance (%)	100 ± 3
<b>Global release (%)</b>	<b>0</b>

The global release corresponds to the difference between the activity of the UiO-66-NH<sub>2</sub> before and after irradiation (<sup>60</sup>Co Source), and it is expressed in percentage of the activity loaded in the MOF before irradiation. The global release is 0%. This result shows that UiO-66-NH<sub>2</sub> has very good irreversible trapping capacities for molecular iodine. The same behavior was observed using UiO-66-NH<sub>2</sub> with prior radiation/moisture exposure (irradiation of 2MGy then steam at 80°C during 7 days).

After the irradiation test, the irradiated UiO-66-NH<sub>2</sub> sample from the first holder (MOF1) were stored separately in a closed plastic bottle for a decay period of eight months to reach the total decay of iodine 131. After this delay, it appeared that most of the UiO-66-NH<sub>2</sub> beads kept their spherical geometry (Fig. 5) along with a slightly improved compressive mechanical strength ( $0.5 \pm 0.2$  N) (Fig. S20). PXRD analyses of granules issued from MOF1 holder (Fig S12) did not show any additional peak nor modification of the full width at half maximum of the Bragg peaks. N<sub>2</sub> physisorption even evidenced a slight increase of porosity (+3%, Table S1). All these results reflect a good stability of the shaped bodies after exposure to iodine, irradiation and stream flow under particularly severe conditions.

## CONCLUSION

In this paper, we studied the immobilization of molecular gaseous radioactive iodine ( $^{131}\text{I}$ ) within the network of a porous MOF material (here UiO-66-NH<sub>2</sub>), under conditions representative of a severe nuclear accident.

To adapt the MOF sample (classically in the form of fine powder) to the filtration lines, and to analyze the performance from the UiO-66-NH<sub>2</sub> phase (and not from any other additional materials), we developed an original binderless granulation method for MOF shaping. This approach, using volatile solvent (H<sub>2</sub>O + ethanol) for the granulation of UiO-66-NH<sub>2</sub>, allows for the production of spherical granules of sufficient mechanical stability for their use in filtration column, under severe flowing conditions (temperature, pressure and high relative humidity). Particles have demonstrated great stability under steam at 100°C during 7 days as well as after having being submitted to very high doses of ionizing radiation (2 MGy,  $\gamma$  radiation from  $^{60}\text{Co}$  source). Even under such drastic conditions, UiO-66-NH<sub>2</sub> material does not exhibit any structural degradation, and improvement of porosity, associated to the removal of residual DMF species obstructing the pores, is even observed. Thanks to this stability, UiO-66-NH<sub>2</sub> granules charged with radioiodine ( $^{131}\text{I}$ ) were placed in a filtration line allowing to mimic the conditions encountered during nuclear accident. After 30 hours at 120°C, under pressure (3.5 bars abs.), and applying a continuous air flow with a relative humidity of 20%, we did not observe any loss of iodine from the filter containing UiO-66-NH<sub>2</sub>. The results presented in this work highlight the potential of MOF materials as filtration medium, to prevent the release of volatile radionuclides issued from nuclear accident. Whereas radioactive gaseous molecular iodine I<sub>2</sub> (mainly from  $^{129/131}\text{I}$ ) remains one of the most radiotoxic species disseminated in the case of a nuclear accident, other highly volatile and toxic molecules containing iodine exist, such as iodomethane. The capture and the immobilization of organo-iodines cannot be ruled out during a nuclear severe accident and their affinity with MOFs under severe conditions needs to be regarded.

## ACKNOWLEDGMENTS

The research leading to these results has been partly supported by the French State under the program "Investissements d'Avenir" called MIRE, managed by the National Research

Agency (ANR) under grant agreement n° ANR-11-RSNR-0013-01. Chevreul Institute (FR 2638), Ministère de l'Enseignement Supérieur et de la Recherche, Région Hauts de France and FEDER are acknowledged for supporting and funding partially this work.

1. M. Baba, *Radiat. Meas.*, 2013, **55**, 17-21.
2. M. Bal, R. C. Jose and B. C. Meikap, *Nucl. Eng. Technol.*, 2019, **51**, 931-942.
3. D. Jacquemain, *NEA/CSNI/R(2014)7*, 2014.
4. B. Azambre, M. Chebbi, O. Leroy and L. Cantrel, *Ind. Eng. Chem. Res.*, 2018, **57**, 1478-1479.
5. M. Chebbi, B. Azambre, L. Cantrel, M. Hove and T. Albiol, *Microporous and Mesoporous Materials*, 2017, **244**, 137-150.
6. T. M. Nenoff, M. A. Rodriguez, N. R. Soelberg and K. W. Chapman, *Microporous Mesoporous Mater.*, 2014, **200**, 297-303.
7. K. W. Chapman, P. J. Chupas and T. M. Nenoff, *J. Am. Chem. Soc.*, 2010, **132**, 8897-8899.
8. M. Chebbi, S. Chibani, J. F. Paul, L. Cantrel and M. Badawi, *Micropor. Mesopor. Mat.*, 2017, **239**, 111-122.
9. S. Chibani, M. Badawi, T. Loiseau, C. Volkringer, L. Cantrel and J. F. Paul, *PhysChemChemPhys*, 2018, **20**, 16770-16776.
10. W. Xie, D. Cui, S. R. Zhang, Y. H. Xu and D. L. Jiang, *Mater. Horiz.*, 2019, **6**, 1571-1595.
11. H. X. Deng, S. Grunder, K. E. Cordova, C. Valente, H. Furukawa, M. Hmadeh, F. Gandara, A. C. Whalley, Z. Liu, S. Asahina, H. Kazumori, M. O'Keeffe, O. Terasaki, J. F. Stoddart and O. M. Yaghi, *Science*, 2012, **336**, 1018-1023.
12. I. M. Honicke, I. Senkovska, V. Bon, I. A. Baburin, N. Bonisch, S. Raschke, J. D. Evans and S. Kaskel, *Angew. Chem. Int. Ed.*, 2018, **57**, 13780-13783.
13. C. Healy, K. M. Patil, B. H. Wilson, L. Hermanspahn, N. C. Harvey-Reid, B. I. Howard, C. Kleinjan, J. Kolien, F. Payet, S. G. Telfer, P. E. Kruger and T. D. Bennett, *Coord. Chem. Rev.*, 2020, **419**.
14. N. C. Burtch, H. Jasuja and K. S. Walton, *Chem. Rev.*, 2014, **114**, 10575-10612.
15. R. Giovine, F. Pourpoint, S. Duval, O. Lafon, J. P. Arnoureaux, T. Loiseau and C. Volkringer, *Cryst. Growth Des.*, 2018, **18**, 6681-6693.
16. C. Volkringer, C. Falaise, P. Devaux, R. Giovine, V. Stevenson, F. Pourpoint, O. Lafon, M. Osmond, C. Jeanjacques, B. Marcillaud, J. C. Sabroux and T. Loiseau, *Chem. Commun.*, 2016, **52**, 12502--12505.
17. S. L. Hanna, D. X. Rademacher, D. J. Hanson, T. Islamoglu, A. K. Olszewski, T. M. Nenoff and O. K. Farha, *Ind. Eng. Chem. Res.*, 2020, **59**, 7520-7526.
18. D. F. Sava, M. A. Rodriguez, K. W. Chapman, P. J. Chupas, J. A. Greathouse, P. S. Crozier and T. M. Nenoff, *J. Am. Chem. Soc.*, 2011, **133**, 12398-12401.
19. C. Falaise, C. Volkringer, J. Facqueur, T. Bousquet, L. Gasnot and T. Loiseau, *Chem. Commun.*, 2013, **49**, 10320-10322.
20. S. Kobinata and S. Nagakura, *J. Am. Chem. Soc.*, 1966, **88**, 3905-&.
21. K. W. Chapman, D. F. Sava, G. J. Halder, P. J. Chupas and T. M. Nenoff, *J. Am. Chem. Soc.*, 2011, **133**, 18583-18585.
22. D. F. Sava, T. J. Garino and T. M. Nenoff, *Ind. Eng. Chem. Res.*, 2012, **51**, 612-618.

23. I. Pakamore, J. Rousseau, C. Rousseau, E. Monflier and P. A. Szilagyi, *Green Chem.*, 2018, **20**, 5292-5298.
24. J. B. DeCoste, G. W. Peterson, H. Jasuja, T. G. Glover, Y. G. Huang and K. S. Walton, *J. Mater. Chem. A*, 2013, **1**, 5642-5650.
25. M. Kandiah, M. H. Nilsen, S. Usseglio, S. Jakobsen, U. Olsbye, M. Tilset, C. Larabi, E. A. Quadrelli, F. Bonino and K. P. Lillerud, *Chem. Mater.*, 2010, **22**, 6632-6640.
26. S. J. Garibay and S. M. Cohen, *Chem. Commun.*, 2010, **46**, 7700-7702.
27. J. H. Cavka, S. Jakobsen, U. Olsbye, N. Guillou, C. Lamberti, S. Bordiga and K. P. Lillerud, *J. Am. Chem. Soc.*, 2008, **130**, 13850-13851.
28. H. X. Sun, P. Q. La, Z. Q. Zhu, W. D. Liang, B. P. Yang and A. Li, *J. Mater. Sci.*, 2015, **50**, 7326-7332.
29. S. Dushman, *J. Phys. Chem.*, 1904, **8**, 453-482.
30. D. Bazer-Bachi, L. Assie, V. Lecocq, B. Harbuzaru and V. Falk, *Powder Technol.*, 2014, **255**, 52-59.
31. B. Valizadeh, T. N. Nguyen and K. C. Stylianou, *Polyhedron*, 2018, **145**, 1-15.
32. X. M. Liu, L. H. Xie and Y. F. Wu, *Inorg. Chem. Front.*, 2020, **7**, 2840-2866.
33. M. Rubio-Martinez, C. Avci-Camur, A. W. Thornton, I. Imaz, D. Maspocho and M. R. Hill, *Chem. Soc. Rev.*, 2017, **46**, 3453-3480.
34. K. U. Ingold and D. A. Pratt, *Chem. Rev.*, 2014, **114**, 9022-9046.



## Highlights

- First example of the capture of radiotoxic  $^{131}\text{I}$  isotope in a MOF
- Confinement of  $^{131}\text{I}$  in UiO-66-NH<sub>2</sub> under conditions representative of nuclear accident (irradiation, temperature, steam)
- Stability of UiO-66-NH<sub>2</sub> under gamma irradiation
- Original binderless method for MOF shaping

## Credit Author Statement

Maeva LELOIRE: Resources, investigation

Jeremy DHAINAUT: investigation, writing-review & editing

Philippe DEVAUX: Resources, Investigation

Olivia LEROY: investigation, writing-review & editing

Hortense DESJONQUERES: investigation, writing-review & editing

Stephane POIRIER: Investigation

Philippe NERISSON: Supervision

Laurent CANTREL: Funding acquisition, project administration

Sébastien ROYER: writing-review & editing

Thierry LOISEAU: Supervision, writing-review & editing

Christophe VOLKRNGER: Conceptualization, project administration, writing original draft, supervision

**Declaration of interests**

☒ The authors declare that they have no known competing financial interests or personal relationships that could have appeared to influence the work reported in this paper.

☐ The authors declare the following financial interests/personal relationships which may be considered as potential competing interests:

## Graphical abstract

